Firing pattern classification and phenotyping in a knowledge base of hippocampal neuron types

Abbreviated title: Firing patterns of hippocampal neurons

Author names and affiliation, including postal codes

Alexander O. Komendantov, Siva Venkadesh, Christopher L. Rees, Diek W. Wheeler, David J. Hamilton, Giorgio A. Ascoli

Krasnow Institute for Advanced Study, George Mason University, 4400 University Drive, MS 2A1, Fairfax, Virginia 2230

Corresponding author(s) with complete address, including an email address and postal code

Alexander O. Komendantov (akomenda@gmu.edu)

Giorgio A. Ascoli (ascoli@gmu.edu)

Krasnow Institute for Advanced Study, George Mason University, 4400 University Drive, MS 2A1, Fairfax, Virginia 2230

Number of pages: 57

Number of figures: 9

Number of tables: 3 (including Box 1)

Number of multimedia: 0

Number of 3D models: 0

Number of words in Abstract: 242

Number of words in Introduction: 618

Number of words in Discussion: 1346

Acknowledgements

This work was supported by grants from the National Institutes of Health (NS39600) and the National Science Foundation (IIS-1302256). We thank Charise M. White and Keivan Moradi for useful discussions and Amar Gawade for help with the web portal. The authors declare no competing financial interests.

Abstract

Systematically organizing the structural, molecular, and physiological properties of hippocampal neurons is important for understanding their computational functions in the cortical circuit. Hippocampome.org identifies 122 neuron types in the rodent hippocampal formation (dentate gyrus, CA3, CA2, CA1, subiculum, and entorhinal cortex) based on their somatic, axonal, and dendritic locations, putative excitatory/inhibitory outputs, molecular marker expression, and basic electrophysiological properties. Here we augment the electrophysiological data of this knowledge base by collecting, quantifying, and analyzing the firing responses to depolarizing current injections for every hippocampal neuron type from available published experiments. We designed and implemented objective protocols to classify

firing responses based on both transient and steady-state activity. Specifically, we identified 5 transients (delay, adapting spiking, rapidly adapting spiking, transient stuttering, and transient slow-wave bursting) and 4 steady states (non-adapting spiking, persistent stuttering, persistent slow-wave bursting, and silence). Leveraging this automated classification approach, we characterized the set of all firing responses reported for each hippocampal neuron type and defined 10 unique firing pattern phenotypes that reveal potential new neuronal subtypes. Several novel statistical associations emerge between firing responses and electrophysiological properties, morphological features, and molecular marker expression. The firing pattern parameters, stimulus conditions, digitized spike times, detailed reference to the original experimental evidence, and analysis scripts are released open-source through Hippocampome.org for all neuron types, greatly enhancing the existing search and browse capabilities. Collating this information online in human- and machine-accessible form will help design and interpret both experiments and hippocampal model simulations.

SIGNIFICANCE STATEMENT

Comprehensive classification of neurons is essential for understanding the functions of neuronal networks. Firing patterns are significant identification characteristics of a neuron and play an important role in information coding in neural systems. Utilizing groundwork laid by Hippocampome.org, a knowledge base characterizing 122 neuron types in the rodent hippocampus, we developed and implemented protocols to classify all known firing responses exhibited by each type based on analysis of transient and

steady-state activity. Leveraging an automated classification approach, we identified 10 unique firing pattern phenotypes and revealed statistical associations of firing responses with electrophysiological properties, morphological features, and molecular marker expressions. The resulting, augmented knowledge base is a powerful tool for designing and interpreting experiments and hippocampal model development.

Introduction

Neuroscience research produces an immense and constantly growing quantity of experimental data and publications. Comprehensive classification of neurons is essential for understanding the functions of neuronal networks at different hierarchical levels. The hippocampus provides an excellent test-bed for this exploration as it is one of the most intensively studied parts of the mammalian brain, which is responsible for learning (Rudy and Sutherland, 1989, 1995), memory (Eichenbaum et al., 1992; Eichenbaum, 2000, 2017), spatial navigation (Hafting et al. 2005; O'Keefe and Dostrovsky, 1971), and emotional associations (Buchanan, 2007).

The Hippocampome.org knowledge base identifies neuron types based on the locations of their somata, axons, and dendrites across 26 hippocampal-formation parcels, putative excitatory/inhibitory character, synaptic selectivity, and major and aligned differences in molecular marker expressions and biophysical properties (Wheeler et al., 2015). Version 1.2 of Hippocampome.org identified 122 neuron types in the 6 areas of the rodent hippocampal formation: 18 in dentate gyrus (DG), 25 in CA3, 5 in CA2, 40 in CA1, 3 in subiculum (SUB), and 31 in entorhinal cortex (EC). The core

assumption of the developed identification scheme is that neurons with different axonal or dendritic patterns belong to different types, but multiple substantial differences in other dimensions may also reveal distinct neuron types. For the majority of neuron types, Hippocampome.org reports 10 basic biophysical parameters that numerically characterize passive and spike properties (hippocampome.org/ephys-defs).

Transmission of information between neurons and, by extension, neuron types is carried out by sequences of action potentials (APs), and the neuronal firing rates are commonly believed to represent the intensity of input stimuli. Since the first discovery in sensory neurons (Adrian and Zotterman, 1926), this principle was generalized and extended to neurons from different brain regions including the hippocampus (McNaughton et al, 1983). However, it was also found that the firing rate of certain neurons may not be constant over time, even if the stimulus is permanently applied. One form of such time-dependent responses is spike frequency adaptation manifested in a decrease of firing rate (Adrian and Zotterman, 1926). Neurons can produce diverse firing patterns in response to similar stimuli due to the inhomogeneity in their intrinsic properties (Connors and Gutnick 1990). Both firing rates and temporal firing patterns are now recognized to play important roles in coding of information in neural systems (Ferster and Spruston 1995).

In electrophysiological experiments *in vitro*, hippocampal neurons demonstrate a vast diversity of firing patterns in response to depolarizing current injections. These patterns are referred to by many names, including delayed, adapting, accommodating, interrupted spiking, stuttering, and bursting (Canto and Witter 2012a,b; Hemond et al., 2008; Lübke et al, 1998; Mercer et al., 2007; Pawelzik et al., 2002; Tricoire et al., 2011).

Uncertainties and ambiguities in classification and naming of neuronal firing patterns are similar to other terminological inconsistencies, which are widely spread in neuroscience literature and pose obstacles to effective communication within and across fields (Hamilton et al., 2017).

In recent years, several efforts have been made aiming to develop general firing pattern classification and to use it for identification of distinct electrical types of cortical neurons (Markram et al., 2004, 2015; Petilla Interneuron Nomenclature Group et al., 2008). A refinement of the Petilla Interneuron Nomenclature was made using statistical analysis of a large set of electrical features of cortical interneurons with different firing patterns (Druckmann et al., 2013), however, the manual classification based on subjectively qualitative or intuitive criteria still have limitations and bias.

In this work, we developed an objective, numerically based automated classification protocol, applied it to available published electrophysiological recordings from identified hippocampal neurons, extended Hippocampome.org with classified firing patterns and their parameters, and uncovered firing pattern phenotypes, potential neuronal subtypes, and statistical associations between firing responses and other neuron type properties.

Materials and Methods

Firing pattern classification methods and algorithms

From the dynamic point of view, firing responses consist of simple or complex transients and steady states. Transients and steady states can be categorized into similar groups of firing pattern elements based on the expression of delay, spike

frequency adaptation or acceleration, slow wave of membrane potential, and interruption of spiking. Figure 1 shows the proposed hierarchy of firing pattern elements and Figure 2 exemplifies the firing pattern elements observed in different hippocampal neuron types. From the variety of transients, we differentiated six firing pattern elements including delay (D), adapting spiking (ASP), rapidly adapting spiking (RASP), transient stuttering (TSTUT), transient slow-wave bursting (TSWB), and accelerating spiking (ACSP). We also distinguished four possible steady state neuronal responses to stimulation: silence (SLN), non-adapting spiking (NASP), and two interrupted firing: persistent stuttering (PSTUT) and persistent slow-wave bursting (PSWB). Simple firing patterns were composed of a single firing pattern element (NASP, PSTUT or PSWB). Complex firing patterns were introduced as a sequence of two or more firing pattern elements with dot-notation (e.g. delayed non-adapting spiking was represented as D.NASP, silence preceded by adapting spiking as ASP.SLN, and non-adapting spiking preceded by delayed transient slow-wave bursting as D.TSWB.NASP). Experimental recordings without identifiable steady states were classified as uncompleted firing patterns (e.g. ASP., D.ASP., or RASP.ASP.).

[Figure 1 is near here]

[Figure 2 is near here]

Table 1 summarizes the principles of classification for firing pattern elements. The transient response was classified as delayed (D) if the latency to the first spike was longer than the sum of the first two interspike intervals (ISI_1 and ISI_2). Similarly, post-firing silence (PFS) was considered to be a steady state (SLN) if it exceeded the sum of

the last two interspike intervals (ISI_{n-1} and ISI_n). In addition, post-firing silence had to last at least twice the longest interspike interval (ISI_{max}).

A persistent firing response with relatively equal interspike intervals denotes non-adapting spiking (NASP); in contrast, transients with a progressive increase or decrease of ISIs can be classified as adapting or accelerating spiking, respectively. To discriminate among several possible combinations of these firing patterns quantitatively and reproducibly, we devised a minimum information description criterion by comparing piecewise (segmented) linear regression models of increasing complexity. Specifically, non-adapting spiking (NASP) can be described by a single parameter, namely the (average) firing rate ($Y=c$). Similarly, fitting normalized interspike intervals versus normalized time with a (2-parameter) linear function $Y=aX+b$ (with $a>0$) corresponds to adapting spiking (ASP.). Fitting data with a piecewise linear function

$$Y = \begin{cases} a_1 X + b_1 & if\ X < \dfrac{b_2 - b_1}{a_1 - a_2} \\ a_2 X + b_2 & if\ X \geq \dfrac{b_2 - b_1}{a_1 - a_2} \end{cases}$$

corresponds to adapting-non-adapting spiking (ASP.NASP) when $a_1>0$ and $a_2=0$ (3 parameters), and to adapting-adapting spiking with different adaptation rates (ASP.ASP.) when both $a_1>0$ and $a_2>0$ (4 parameters). We selected a model with fewer parameters if increasing the number of parameters did not provide a statistically significant better fit than a less complex model. The significance level for the differences between one-parameter fitting (NASP) and two-parameter linear-regression fitting

(ASP.) was less than 0.05. In order to avoid very weak adaptations from being identified as ASP., a minimum threshold of 0.003 was used for the slope a_1.

[Table 1 is near here]

For the next stage of comparison, we used a Bonferroni correction for the *p*-value for the differences between two-parameter linear-regression fitting (ASP.) and three-parameter piecewise-linear-regression fitting (ASP.NASP). Specifically, in order for a pattern with an adapting spiking transient (i.e. ASP.) to be qualified as ASP.NASP, the *p*-value must be less than 0.025. Similarly, the *p*-value for the differences between three-parameter piecewise-linear-regression fitting (ASP.NASP) and four-parameter piecewise-linear-regression fitting (ASP.ASP.) must be less than 0.016. Examples of fitting spiking activity with linear regression and piecewise linear regression models are presented in Figure 3. If adaptation was only observed in the first two or three ISIs in a long train of spikes, and if the linear fitting of slope a_1 exceeded 0.2, then this transient was classified as rapidly adapting spiking (RASP.). For accelerating spiking (ACSP.), the linear fitting slope must be negative.

[Figure 3 is near here]

We defined transient stuttering (TSTUT) as a short high-frequency (>25 Hz) cluster of APs followed by other distinctive activity. In addition, the first ISI after a TSTUT cluster must be 2.5 times longer than the last ISI of the cluster and 1.5 times longer than the next ISI. Under transient slow-wave bursting activity (TSWB), a cluster of two or more spikes rides on a slow depolarization wave (>5mV) followed by a strong slow AHP. Persistent stuttering (PSTUT) was classified as firing activity with high-frequency clusters of action potentials separated by relatively long silence intervals.

According to our definition, each of the silence intervals must be more than 5 times longer than the sum of the previous ISI and the next ISI. Similarly, under persistent slow-wave bursting (PSWB) activity, these clusters of two or more tightly grouped spikes ride on slow depolarizing waves (>5 mV) followed by strong, slow AHPs.

Experimental Design and Statistical Analysis

Data collection, extraction and digitization

The firing patterns of hippocampal neurons were classified based on their spiking responses to supra-threshold step-current pulses of different amplitude and duration. We extracted values of first spike latency (i.e. delay), interspike intervals (ISIs) and post-firing silence (in ms). In addition, the slow-wave amplitude (in mV) was extracted from burst firing recording. Firing pattern parameters were extracted from electronic figures using Plot Digitizer (plotdigitizer.sourceforge.net) for all 89 Hippocampome.org neuron types (Wheeler et al., 2015) for which they were available. For firing pattern identification and analysis, ISIs in each recording were normalized to the shortest interspike interval (ISI_{min}) within that time series to allow meaningful comparison.

Implementation of firing pattern classification algorithms

The automated firing-pattern classification algorithms are implemented in Microsoft Excel using Solver and the Data Analysis Toolbox (F-test and t-test) to perform piecewise linear fitting and statistical tests (Fig. 4). They also are implemented in the Java programming language using the Apache Commons Mathematics Library (http://commons.apache.org/proper/commons-math). The Java implementation is

available as an open source at https://github.com/Hippocampome-Org/NeuroSpikePatterns.

[Figure 4 is near here]

Representation of firing patterns in the database and web portal

Hippocampome.org provides access to morphological, molecular, electrophysiological, connectivity, and firing pattern information for 122 neuron types. Amassed firing pattern information includes figures with recordings, the duration and amplitude of stimulation, digitized interspike intervals, firing pattern parameters, and the result of the firing pattern classification algorithm detailed here. The implementation of Hippocampome.org supports the model-view-control software design. The model component defines the database interface and is provided solely by server-side code. The view component rendering the web pages and the control code implementing the decision logic are both served up by the server, but are run in the user's browser. The underlying relational database ensures flexibility in establishing relations between data records.

Hippocampome.org is deployed on a CentOS 5.11 server running Apache 2.2.22 and runs on current versions of several web browsers (Mozilla Firefox, Google Chrome, Apple Safari, and Microsoft Internet Explorer). Knowledge base content is served up to the PHP 5.3.27 website from a MySQL 5.1.73 database. Django 1.7.1 and Python 3.4.2 provide database ingest capability of comma separated value annotation files derived from human-interpreted peer-reviewed literature. Hippocampome.org code is available at https://github.com/Hippocampome-Org.

Pairwise correlation analysis

We explored pairwise correlations between all observed firing patterns, firing pattern elements, and 316 properties of Hippocampome.org neuron types, including: primary neurotransmitter; axonal, dendritic, and somatic locations in the 26 parcels and 6 sub-regions of the hippocampal formation; the projecting (inter-area) or local (intra-area) nature of axons and dendrites; axon and dendrite co-presence within any partition; axonal and dendritic presence in a single layer only or in ≥3 layers; clear positive or negative expression of any biomarkers; high (top third) or low (bottom third) values for electrophysiological properties (Wheeler et al., 2015); and connectivity patterns and superpatterns (Rees et al., 2016). To evaluate the correlations between these categorical properties, we used 2 × 2 contingency matrices with Barnard's exact test (Barnard, 1947), which provides the greatest statistical power when row and column totals are free to vary (Lydersen et al., 2009). The correlation analysis is implemented in Matlab (MathWorks, Inc.).

Cluster analysis

We conducted a cluster analysis of numerical electrophysiological data, such as the width of action potential and the minimum interspike interval, as well as categorical firing pattern data. Spike width is most commonly measured as the width at half-maximal spike amplitude (Bean, 2007), as is done in Hippocampome.org (Wheeler et al., 2015). Minimum interspike intervals (ISI_{min}) are extracted from digitized recordings or directly from corresponding papers. We assign weights for categorical firing pattern data according to the formula $W_i=(N-n_i)/N$, where W_i is the weight of firing pattern

element i, n_i is the number of cell types expressing firing pattern(s) with element i, N is the total number of cell types/subtypes, and i={ASP, D, RASP, NASP, PSTUT, PSWB, SLN, TSUT,TSWB}. We employed a two-step cluster analysis using the IBM SPSS Statistics 24 software for statistical analysis. Silhouette measures of cohesion and separation greater than 0.5 indicated that the elements were well matched to their own clusters and poorly matched to neighboring clusters, and that the clustering configuration was appropriate.

Statistical data were expressed as mean ± standard deviation.

Results

Firing pattern matrix and its analysis

Applying firing pattern identification algorithms to all available digitized electrophysiological recording data from 89 neuron types resulted in the detection of 23 different firing patterns. They are presented in the form of a firing pattern matrix (Fig. 5). An interactive online version of the matrix is available at hippocampome.org/firing_patterns.

[Figure 5 is near here]

It is known that some cells can demonstrate different firing patterns with changes of stimulation amplitude. In addition, different cells belonging to the same neuron type often exhibit different firing patterns under the same experimental conditions. Therefore, we specified possible firing pattern subtypes within cell types based on their firing responses and distinguished the following groups of phenotypes: individual types with single behavior, individual types with multiple behaviors, subtypes with single behavior,

subtypes with multiple behaviors, and undetermined cases which may represent subtypes or multiple behaviors.

As one can see from the matrix in Figure 5, the firing patterns have different distributions among neuron types. The total number of neuron types expressing each of the 23 detected firing patterns are shown in a bar diagram (see Fig. 6A).

Firing patterns can be grouped for analysis based on the number of elements that comprise them (e.g. single, like ASP., NASP, PSTUT; double, like ASP.NASP, TSWB.SLN, D.NASP; and triple, like D.RASP.NASP, D.TSWB.NASP), whether they are completed (e.g. NASP, PSTUT, ASP.NASP, ASP.SLN, PSWB) or uncompleted (ASP., RASP.ASP., TSTUT.ASP.), and according to which are most frequent (ASP., NASP), common (PSTUT, ASP.NASP, D.NASP, etc.), and infrequent (TSWB.SLN, D.RASP.NASP,PSTUT, etc.). In addition, we also analyzed the nine firing pattern elements whose distributions are shown in Figure 6B, and we detected three major groups among them: the most frequent (ASP, NASP), common (RASP, SLN, PSUT, D), and infrequent (TSTUT, TSWB, PSWB).

The set of firing patterns exhibited by a given neuron type forms its firing pattern phenotype. Figure 6C shows a pie diagram illustrating the complexity of firing pattern phenotypes of hippocampal neurons. Of those types for which information exists (72%), the largest group is individual types that show a single behavior (26%). The group of “individual types with multiple behaviors” contains 8% of types; the group of simple subtypes and the group of “subtypes AND multi-behavior” each represent 7% of types. The second largest group is composed of cases that may be “subtypes OR multi-behavior” (25%).

Figure 6D presents the relationships between firing pattern elements within the firing patterns of hippocampal neuron types in a form of Venn diagram. Firing pattern elements are illustrated as ellipses. Areas formed by the intersections of overlapping ellipses represent complex firing patterns. Numbers within ellipses and their overlaps mark the number of cell types with specific firing patterns. In these intersections, the following features are evident: for the four main firing transients (ASP., RASP., TSTUT., TSWB.) often end with either NASP or with SLN, ASP. is often preceded by RASP. and occasionally by TSTUT., interrupted steady state firings (PSTUT and PSWB) stand out as a separate group, and delay (D.) most often precedes NASP.

[Figure 6 is near here]

Our classification of firing pattern elements implies the possibility of three single-element firing patterns (NASP, PSTUT, PSWB) and 23 double-element firing patterns consisting of one of four steady states (SLN, NASP, PSTUT, PSWB) preceded by one of six transients (D, ACSP, ASP, RASP, TSTUT, TSWB). Also, five double-transients are possible after an initial delay, resulting in an additional 20 triple-firing patterns. Table 2 shows the occurrences of these 46 completed firing patterns in hippocampal and other neurons. Only 15 of the firing patterns were discovered in literature data for 89 hippocampal neuron types (green shading in Table 2), though 5 additional firing patterns were found in other neurons. ACSP.NASP has been shown in the ventral horn interneuron of turtles (Smith and Perrier 2006), D.PSWB in the cultured rutabaga mutant giant neuron of *Drosophila* (Zhao and Wu 1997), D.ASP.SLN in the neuron of the external lateral subnucleus of the lateral parabrachial nucleus (Hayward and Felder 1999), D.ACSP.NASP in the motoneuron (Leroy et al. 2014), and D.TSUT.SLN in the

striatal fast-spiking neuron (Sciamanna and Wilson 2011)). Also, we categorized 12 firing patterns as “not found but possible” (white shading and black text in Table 2) and 14 firing patterns as “improbable” from a dynamical or physiological point of view (white shading and gray text).

[Table 2 is near here]

Firing pattern phenotypes and their characterization

For simplicity purpose, we determined a firing pattern phenotype on the basis of its constituent firing pattern elements, which received their weights according to frequency of occurrence among 116 neuron types and putative subtypes. As a result of weight assignment (see *Materials and Methods*), infrequent firing pattern elements (PSWB, TSTUT and TSWB) received high weights (0.99, 0.95 and 0.94, respectively), very frequent elements (ASP and NASP) got low weights (0.37 and 0.39), and common elements (D, RASP, PSTUT and SLN) obtained intermediate weights (0.90, 0.76, 0.88 and 0.87). Eleven firing pattern phenotypes identified with two-step cluster analysis can be organized into a seven-level hierarchical binary tree, which is presented in Figure 7A. Most generally, hippocampal neuron types and subtypes can be subdivided into two big groups: neuron types with spiking phenotypes (76%) and those with burst- and stutter-firing phenotypes (24%). Among the neuron types with spiking phenotypes, a group with a delayed spiking phenotype (9% of cell types) can be distinguished. The group with burst- and stutter-firing phenotypes was subdivided into groups of neuron types with bursting (6%) and stuttering phenotypes (18%). In turn, the bursting group contains persistent bursting (1%) and non-persistent bursting (5%) phenotypes.

Similarly, the stuttering group includes neurons types with persistent stuttering (12%) and non-persistent stuttering (6%) phenotypes. Besides delayed spiking neurons, there is a large group of non-delayed spiking neuron types (67%) that is subdivided into the group with non-adapting spiking (11%) and the group with adapting spiking phenotypes (56%). The latter group can be subdivided into rapidly adapting (21%) and normally adapting spiking phenotypes (35%). The rapidly adapting group consists of neuron types with RASP-ASP (15%) and RASP-NASP (6%) phenotypes; the normally adapting group includes the group with the continuous adapting spiking phenotypes (29%) and neuron types with discontinuous adapting spiking phenotype (7%), for which the silent steady state is typical. The group of continuous adapting spiking neurons can be subdivided into adapting-non-adapting spiking (14%) and simple adapting spiking (15%) phenotypes. However, the last of the groups is the incomplete phenotype, because a steady state that was not experimentally recorded could be either NASP or SLN. Thus, simple adapting spiking could be adapting-non-adapting spiking or discontinuous adapting spiking, and the total number of phenotypes could be potentially reduced to ten. This division of the adapting spiking groups reflects differences in adaptation rates, duration, and subsequent steady states.

Each sector of the circular diagram in Figure 7B shows the percentage of neuron-types with the corresponding firing pattern phenotype within the whole set of 116 neuron types/subtypes. Certain phenotypes (e.g. persistent bursting, non-persistent bursting and rapidly adapting – non-adapting spiking) are composed predominantly of excitatory neuron types (100%, 83% and 83%, respectively). Conversely, persistent stuttering, delayed spiking, non-adapting spiking and simple adapting spiking are

phenotypes composed largely by inhibitory neuron types (93%, 70%, 77% and 71%, respectively). Non-persistent stuttering, adapting–non-adapting spiking, discontinuous adapting spiking and rapidly adapting–adapting spiking phenotypes have equal or comparably equal numbers of excitatory and inhibitory neuron types.

Figure 7C displays the percentage of occurrences of firing pattern elements in firing pattern phenotypes; 100% indicates that defining firing pattern elements are observed in all cell types of a phenotype, while non-defining firing pattern elements range from 8% to 82%. For example, D is the defining element for delayed spiking, PSTUT for persistent stuttering, ASP and SLN for discontinuous adapting spiking, and ASP and NASP for adapting-non-adapting spiking. Each of the four major elements of interrupted firing patterns (PSWB, PSTUT, TSWB and TSTUT) is observed in a single firing pattern phenotype (persistent bursting, non-persistent bursting, persistent stuttering, and non-persistent stuttering, respectively). Other firing pattern elements (D, RASP, ASP, NASP, and SLN) appear in several firing pattern phenotypes.

As shown in the three-dimensional column chart in Figure 7D, the firing pattern phenotypes have different distributions among all neuron types/subtypes in the sub-regions of the hippocampal formation. The PSTUT (50%) and NASP (54%) phenotypes are more common in CA1, delayed spiking is most common phenotype in DG (50%), and ASP-NASP (50%), discontinuous ASP (50%), RASP-NASP (71%), and RASP-ASP (47%) occurred more often in EC than in other areas. There are no clear expressed tendencies in simple ASP, non-persistent bursting, and non-persistent stuttering phenotypes distributions; PSWB is presented by just a single type (CA3 Pyramidal cell).

[Figure 7 is near here]

Usage of information from Hippocampome.org

Searching and Browsing

The addition of firing pattern information to Hippocampome.org extends opportunities for broad-scope analytics and quick-use checks of neuron types. Similar to morphological, molecular, and electrophysiological information, firing pattern information can be browsed with the online version of the matrix presented in Figure 5 or searched with queries containing AND & OR Boolean connectors (see Hippocampome.org →Search → Neuron Type). Figure 8A shows a sample search for neuron types with combinations of molecular (CB-negative), morphological (axons in CA1 stratum pyramidale), electrophysiological (AP_{width} < 0.96 ms), and firing pattern properties (PSTUT firing, $\frac{ISI_i^{max}}{ISI_{i+1}} > 10$), which is represented schematically in the form of a Venn diagram. Each ellipse symbolically represents a set of neuron types with a distinct property, and intersections of several sets or overlapping regions represent neuron types with several properties. In the presented example, the compound search led to a single result: only CA1 Axo-axonic neurons express all five selected properties.

Browsing (i.e. by clicking on this result) leads to the Neuron Page (Fig. 8B) where all information associated with a given neuron type is amassed, including synonyms, morphology, electrophysiological parameters, molecular markers, synaptic connectivity, and firing patterns. Every property, including firing patterns, on the Neuron Page links to an evidence page that lists all supporting bibliographic citations, complete with extracted quotes, figures (Fig. 8C), tables with all firing pattern parameters (Fig. 8D), and interspike intervals.

[Figure 8 is near here]

The portal also provides authors' original firing pattern name descriptions, when available (see Hippocampome.org → Search → Original Firing Pattern).

Statistical analysis of categorical data

Firing pattern information extends the Hippocampome.org knowledge base capacity to more than 27,000 pieces of knowledge, and it allows the unearthing of hidden relationships between electrophysiological, molecular, morphological, and firing data in hippocampal neurons, which are difficult to find amongst the large body of literature. Statistical co-occurrence of categorical data was analyzed with contingency tables. For this analysis, numerical electrophysiological parameters were converted to categorical variables by labeling values as high or low in the top and bottom one-third of the range, respectively; thus, only very high and very low values were analyzed. Several interesting examples of such findings are presented in Box 1. For example, positive expression of cholecystokinin (CCK) tends to co-occur with adapting spiking (ASP.) ($p<0.011$ with Barnard's exact test from all $n = 26$ pieces of evidence). Moreover, neuron types with high input resistance (R_{in}) do not display adapting spiking ($p<0.012$, $n=35$), and, of the 25 neuron types that have narrow APs, only CA1 Basket CCK+ display rapidly adapting spiking (RASP.) ($p<0.008$, $n=25$).

[Box 1 is near here]

Analysis of numerical electrophysiological data

Hippocampome.org contains characteristics of neuron types which are important for electrophysiological classifications (Druckmann et al., 2013; Tripathy et al., 2015). These data allow to study the correlations between electrical parameters and firing pattern characteristics, for example, the relationship between action potential width (AP_{width}) and the minimum of interspike intervals (ISI_{min}). Figure 9 shows an AP_{width} plotted against ISI_{min} in a scatter diagram (panel A) for 81 neuron types and subtypes for which both parameters are available. Corresponding AP_{width} histogram (panel B) and ISI_{min} histogram (panel C) demonstrate polymodal distributions. Analysis of the scatter plot and distributions reveals several distinct groups of neuron types/subtypes. The horizontal dashed line (ISI_{min}=34 ms) separates 9 neurons with slow spikes from 72 neurons with fast and moderate spikes. Eighty-nine percent of neurons with slow spikes are excitatory; 61% of neurons with slow and moderate spikes are inhibitory. For the last group, a general trend of ISI_{min} rise with increasing of AP_{width} is observed (black dashed line in panel A). This trend was adequately fitted with a linear function $Y = 13.79X - 0.05$ ($R^2 = 0.52$). The opposite trend is seen within the group with slow spikes, which was fitted with a decreasing linear function $Y = - 26.72X + 76.42$ ($R^2 = 0.83$). The correlations for these trends are highly significant. In turn, the neuron types can be separated by spike width. The vertical dashed lines *w1* (AP_{width}=0.73 ms) and *w2* (AP_{width}=1.12 ms) separate neuron types with narrow, medium and wide action potentials. The group of neuron types with narrow spikes (n=22) includes only inhibitory neurons which have AP_{width} in the range from 0.20 to 0.73 ms (0.54 ± 0.12 ms). In contrast to this, the group of neuron types with wide spikes (n=28) contains only excitatory neurons with AP_{width} in the range from 1.13 to 2.10 ms (1.49 ± 0.23 ms). The

group of neuron types with medium spikes (n = 31) with AP_{width} range from 0.74 to 1.12 ms (0.89 ± 0.12 ms) includes predominantly inhibitory (74%) and some excitatory (26%) neurons.

[Figure 9 is near here]

Hippocampome.org data also allow to reveal how firing patterns and firing pattern phenotypes distributed among neuron types with different electrophysiological characteristics. For example, among 22 neuron types/subtypes from the group with AP_{width}<0.72 ms, 13 cell types demonstrated so-called fast spiking behavior which is distinguished by narrow spikes, high firing rate and the absence or weak expression of spike frequency adaptation (Jonas et al., 2004). Five of the 13 neuron types belong to PSUT firing pattern phenotypes (i.e. CA3 Trilaminar (Gloveli et al., 2005), CA3 Aspiny Lucidum ORAX (Spruston et al., 1997), CA2 Basket (Mercer et al., 2007), CA1 Axo-axonic (Pawelzik et al., 2002), CA1 Radial Trilaminar (Tricoire et al, 2011)); 3 types belong to the NASP phenotype (DG Basket (Savanthrapadian et al., 2014), CA1 Horizontal Axo-axonic (Tricoire et al, 2011), EC MEC LIII Superficial Multipolar Interneuron (Kumar and Buckmaster 2006)); 2 types belong to the simple adapting spiking phenotype (CA3 Axo-axonic (Dugladze et al., 2012), CA2 Bistratified (Mercer et al., 2007)); two types belong to the ASP-NASP phenotype (DG HICAP (Mott et al., 1997), DG AIPRIM (Lubke et al, 1998; Scharfman 1992)); and 1 type belongs to non-persistent stuttering phenotype (CA1 basket (Lee et al., 2011)). Firing pattern phenotypes are unequally distributed among group with different electrophysiological characteristics. Persistent and non-persistent stuttering phenotypes and non-persistent bursting phenotypes are composed entirely of neuron types with narrow and medium

fast/moderate spikes. On the other hand, the rapidly adapting – non-adapting spiking phenotype is represented solely by neurons with wide moderate spikes. Other firing pattern phenotypes are composed of varying proportions of neuron types from different electrophysiological groups.

Discussion

Neurons vary from each other by morphological and molecular features including the variety and distribution of ion membrane channels in somata and dendrites. These intrinsic properties determine important physiological functions such as excitability, efficacy of synaptic inputs (Häusser et al., 2000; London et al., 2002; Komendantov and Ascoli, 2009), shapes of individual action potentials, and their frequency (Bean, 2007) and temporal patterns (Mainen and Sejnowski, 1996). Since electrophysiological properties are sufficiently uniform in most types of neurons, as well as morphological and molecular properties (Wheeler et al., 2015), it is quite reasonable use them to refine neuronal classification. In the neuroscience literature, the firing patterns of neuronal activity are commonly used to characterize or identify groups of neurons (e.g. “strongly adapting, normally adapting, and nonadapting cells” (Mott et al., 1997); “fast-spiking and non-fast-spiking” interneurons (Bjorefeldt et al., 2016); “late spiking” cells (Tamas et al., 2003); “stuttering interneurons” (Song et al., 2013); “bursting” and “non-bursting” neurons (Hablitz and Johnston, 1981; Maskawa et al., 1982); “regular spiking, bursting, and fast spiking” (McCormick et al., 1985), etc.). In this study, we show that with a quantitative, numerical approach based on the analysis of transients and steady states of evoked spiking activity, the firing patterns of hippocampal neuronal types can be

readily classified. This work is a further development of the qualitative approach of the Petilla Interneuron Nomenclature Group (2008), which was applied to firing patterns in cortical neurons (Druckmann et al., 2013; Markram et al., 2015). Our data-driven firing pattern classification technique can be used to identify more than 30 patterns. Among electrophysiological recordings from 89 neuron types in the rodent hippocampus, 23 firing patterns were identified, including 15 that were completed (i.e., firing patterns with transient(s) and putative steady state components) (see Figs. 5 and 6). Taking into consideration the firing pattern information allows to improve and clarify neuronal classification by selecting putative electrophysiological subtypes among 18 neuron types. In addition, electrophysiological subtypes are possible for 29 neuron types. Subsequent two-step cluster analysis allows for the clear distinguishing of 10 unique firing pattern phenotypes among 116 hippocampal neuron types and putative subtypes. However, our firing pattern classification framework can be easily applied to spiking activity of neurons from other brain regions. While six of ten firing pattern phenotypes are more typical for excitatory or inhibitory neuron types, four of them are equally mixed (Fig. 7B). Thus, it seems that in many cases, categorization of a firing pattern phenotype by itself is a necessary but insufficient attribute for reliable neuronal electrophysiological identification of neurons.

The frequency of discharges is an important characteristic of neuronal communication. Many neuron types, especially interneurons, show fast spiking behavior: they are capable of firing at high frequencies (200 Hz or more) with little decrease in frequency during prolonged stimulation (Jonas et al., 2004; Bean 2007). Spike frequency correlates with electrophysiological characteristics such as action

potential duration or fast AHP amplitude (Druckmann et al., 2013). Fast spiking neurons typically have narrow action potentials and high amplitude fast AHP (Bean 2007). Our correlation analysis of Hippocampome.org data reveals that non-adapting spiking (NASP) is not inherent in neuron types with extremely wide action potentials or with very low amplitude fast AHPs. Otherwise, rapidly adapting spiking (RASP) is not typical for neurons with very narrow action potentials or with extremely high amplitude fast AHPs (Box 1). When ISI_{min} is plotted against AP_{width} for all neuron types with fast and moderate spikes (ISI_{min} < 34 ms or maximum frequencies more than 29 Hz) and for all neuron types with slow spikes (ISI_{min} > 34 ms or maximum frequencies less than 29 Hz) highly significant linear relationships are observed (Fig. 9A).

The fast spiking phenotype is underlying by a fast delayed rectifier current, which is largely presented in these interneurons (Jonas et al., 2004; Bean 2007). The channels mediating this K^+ current are assembled from Kv3 subunits (Rudy and McBain, 2001). The kinetics for fast AHP provided by these channels appear to be optimal to accelerate recovery of sodium channels from inactivation and to decrease delay in the onset of the AP initiation (Lien and Jonas, 2003). Firing pattern phenotypes of central mammalian neurons are determined by biophysical properties associated with expression and distribution of several types of Ca^{2+} and K^+ channels, which modulate specific ion currents (Bean, 2007), as well as with expression of other molecular markers (Caballero et al., 2014; Markram et al., 2004; Petilla Interneuron Nomenclature Group et al., 2008). Despite the relative sparsity of molecular marker information in the current version of the Hipocampome.org knowledge base (Wheeler et al., 2015), analysis of the correlations between firing patterns and other neuronal properties

reveals interesting statistical peculiarities of molecular marker expression in the hippocampal neuron types (see Box 1 for examples).

Firing patterns play important roles in neural networks including encoding input features, transmitting information or synchronizing activity across different regions. A single spike can provide temporally precise neurotransmitter release, however, in central synapses, this release usually has low probability. Neurons can compensate the unreliability of their synapses by transmitting signals via multiple synaptic endings or repeatedly activate a single synapse (Lisman, 1997). Thus, spikes, which are grouped together in bursting or stuttering activity, increase probability of transmission via unreliable synapses compared to separated spikes with the same average frequency. In the hippocampus, a single burst can produce long-term synaptic modifications (potentiation or depression) (Lisman, 1997). It was hypothesized that, due to the interplay between short-term synaptic depression and facilitation, bursting with certain values of ISIs are more likely to cause a postsynaptic cell to fire than bursts with higher or lower frequencies (Izhikevich et al., 2003). Experimental studies provide strong evidence that different brain circuits employ distinct schemes to encode and transmit information (Xu et al, 2012): while transmission of the information by isolated spikes is insignificant for acquisition of recent contextual memories in the hippocampus, it is essential for memory function in the medial prefrontal cortex. However, even within the hippocampus, different neuronal circuits probably may employ distinct coding schemes by relying on isolated spikes or bursts of spikes for execution of critical functions (Xu et al, 2012). Indeed, distinct sub-regions of the hippocampal formation show differential distributions of firing pattern phenotypes (Fig.7), among which the group of spiking

phenotypes contains the majority of neuron types/subtypes. Parvalbumin (PV) – and cholecystokinin (CCK)-expressing basket cells are most famous examples of spiking interneurons with similar morphology but with different electrophysiological and molecular properties, and functions in the hippocampal networks (Bartos and Elgueta, 2012; Freund and Katona, 2007). Non-adapting spiking (NASP) is typical for fast-spiking PV-positive interneurons, which synaptic terminals open P/Q-type calcium (Cav2.1) channels. In contrast, CCK-positive neurons demonstrate action potentials with adapting firing patterns and selectively open N-type calcium (Cav2.2) channels. The P/Q-type channels are localized at the synaptic active zone to provide precisely timed univesicular release. The N-type channels are distributed throughout the bouton, but not at the active zones, and the axon terminals of CCK-positive neurons have several active zones that allow asynchronous multivesicular release (Freund and Katona, 2007). These properties indicate that CCK-positive neurons may act as slow processing devises, whereas PV-positive neurons act as fast signaling units, which role in gamma oscillogenesis and cognition is well supported (Bartos and Elgueta, 2012).

The information on firing patterns of neuron types has been added to the Hippocampome.org knowledge base that already contained information on morphology, molecular marker expression, connectivity, and other electrophysiological characteristics (Wheeler et al., 2015). Computation of the potential connectivity map of all known 121 neuron types by supplementing available synaptic data with spatial distributions of axons and dendrites allows one to build a network containing more than 3200 connections (Rees et al., 2016). Further directions of Hippocampome.org development include modeling and simulation of firing activity of different neuron types,

quantitative estimation of axonal and dendritic distributions across parcels, neuron count, synaptic profiles and others. All of this makes Hippocampome.org a powerful tool for experimentalists and modelers, especially for development of real-scale models of the hippocampus. Such knowledge bases are very important in view of the growing role of data sharing in neuroscience research.

References

Adrian ED, Zotterman Y (1926) The impulses produced by sensory nerve endings: Part 3. Impulses set up by touch and pressure. J Physiol 61:465-483.

Armstrong C, Szabadics J, Tamás G, Soltesz I (2011) Neurogliaform cells in the molecular layer of the dentate gyrus as feed-forward γ-aminobutyric acidergic modulators of entorhinal-hippocampal interplay. J Comp Neurol519:1476-1491.

Ascoli GA, Brown KM, Calixto E, Card JP, Galván EJ, Perez-Rosello T, Barrionuevo G (2009) Quantitative morphometry of electrophysiologically identified CA3b interneurons reveals robust local geometry and distinct cell classes. J Comp Neurol 515:677-695.

Barnard GA (1947) Significance tests for 2×2 tables. Biometrika 34:123–138.

Bartos M, Elgueta C (2012) Functional characteristics of parvalbumin- and cholecystokinin-expressing basket cells. J Physiol 590:669-681.

Bean BP (2007) The action potential in mammalian central neurons. Nat Rev Neurosci 8:451-465.

Bilkey DK, Schwartzkroin PA (1990) Variation in electrophysiology and morphology of hippocampal CA3 pyramidal cells. Brain Res 514:77-83.

Bjorefeldt A, Wasling P, Zetterberg H, Hanse E (2016) Neuromodulation of fast-spiking and non-fast-spiking hippocampal CA1 interneurons by human cerebrospinal fluid. J Physiol 594:937-952.

Buchanan TW (2007) Retrieval of emotional memories. Psychol Bull 133: 761-779.

Buhl EH, Han ZS, Lörinczi Z, Stezhka VV, Karnup SV, Somogyi P (1994) Physiological properties of anatomically identified axo-axonic cells in the rat hippocampus. J Neurophysiol 71:1289-1307.

Bullis JB, Jones TD, Poolos NP (2007) Reversed somatodendritic I(h) gradient in a class of rat hippocampal neurons with pyramidal morphology. J Physiol 579:431-443.

Caballero A, Flores-Barrera E, Cass DK, Tseng KY (2014) Differential regulation of parvalbumin and calretinin interneurons in the prefrontal cortex during adolescence. Brain Struct Funct 219:395-406.

Canto CB, Witter MP (2012) Cellular properties of principal neurons in the rat entorhinal cortex. I. The lateral entorhinal cortex. Hippocampus 22:1256-1276.

Canto CB, Witter MP (2012) Cellular properties of principal neurons in the rat entorhinal cortex. II. The medial entorhinal cortex. Hippocampus 22:1277-1299.

Chevaleyre V, Siegelbaum SA (2010) Strong CA2 pyramidal neuron synapses define a powerful disynaptic cortico-hippocampal loop. Neuron 66:560-572.

Connors BW, Gutnick MJ (1990) Intrinsic firing patterns of diverse neocortical neurons. Trends Neurosci 13:99-104.

Druckmann S, Hill S, Schürmann F, Markram H, Segev I (2013) A hierarchical structure of cortical interneuron electrical diversity revealed by automated statistical analysis. Cereb Cortex 23:2994-3006.

Dugladze T, Schmitz D, Whittington MA, Vida I, Gloveli T (2012) Segregation of axonal and somatic activity during fast network oscillations. Science 336:1458-1461.

Eichenbaum H (2000) A cortical-hippocampal system for declarative memory. Nat Rev Neurosci 1:41-50.

Eichenbaum H (2017) The role of the hippocampus in navigation is memory. J

Neurophysiol. 117:1785-1796.

Eichenbaum H, Otto T, Cohen NJ (1992) The hippocampus--what does it do? Behav Neural Biol 57:2-36.

Ferster D, Spruston N (1995) Cracking the neuronal code. Science 270:756-757.

Freund TF, Katona I (2007) Perisomatic inhibition. Neuron 56:33-42.

Fuentealba P, Klausberger T, Karayannis T, Suen WY, Huck J, Tomioka R, Rockland K, Capogna M, Studer M, Morales M, Somogyi P (2010) Expression of COUP-TFII nuclear receptor in restricted GABAergic neuronal populations in the adult rat hippocampus. J Neurosci 30:1595-1609.

Gloveli T, Dugladze T, Saha S, Monyer H, Heinemann U, Traub RD, Whittington MA, Buhl EH (2005) Differential involvement of oriens/pyramidale interneurones in hippocampal network oscillations *in vitro*. J Physiol 562:131-147.

Golomb D, Yue C, Yaari Y (2006) Contribution of persistent Na^+ current and M-type K^+ current to somatic bursting in CA1 pyramidal cells: combined experimental and modeling study. J Neurophysiol 96:1912-1926.

Gulyás AI, Szabó GG, Ulbert I, Holderith N, Monyer H, Erdélyi F, Szabó G, Freund TF, Hájos N (2010) Parvalbumin-containing fast-spiking basket cells generate the field

potential oscillations induced by cholinergic receptor activation in the hippocampus. J Neurosci 30:15134-15145.

Hablitz JJ, Johnston D (1981) Endogenous nature of spontaneous bursting in hippocampal pyramidal neurons. Cell Mol Neurobiol 1:325-334.

Hafting T, Fyhn M, Molden S, Moser MB, Moser EI (2005) Microstructure of a spatial map in the entorhinal cortex. Nature 436:801-806.

Hamam BN, Kennedy TE, Alonso A, Amaral DG (2000) Morphological and electrophysiological characteristics of layer V neurons of the rat medial entorhinal cortex. J Comp Neurol 418:457-472.

Hamam BN, Amaral DG, Alonso AA (2002) Morphological and electrophysiological characteristics of layer V neurons of the rat lateral entorhinal cortex. J Comp Neurol 451:45-61.

Hamilton DJ, Wheeler DW, White CM, Rees CL, Komendantov AO, Bergamino M, Ascoli GA (2017) Name-calling in the hippocampus (and beyond): coming to terms with neuron types and properties. Brain Inform 4:1-12.

Häusser M, Spruston N, Stuart GJ (2000) Diversity and dynamics of dendritic signaling. Science 290:739-744.

Hayward LF, Felder RB (1999) Electrophysiological properties of rat lateral parabrachial neurons in vitro. Am J Physiol 276:R696-R706.

Hemond P, Epstein D, Boley A, Migliore M, Ascoli GA, Jaffe DB (2008) Distinct classes of pyramidal cells exhibit mutually exclusive firing patterns in hippocampal area CA3b. Hippocampus 18:411-424.

Izhikevich EM, Desai NS, Walcott EC, Hoppensteadt FC (2003) Bursts as a unit of neural information: selective communication via resonance. Trends Neurosci 26(3):161-167.

Jonas P, Bischofberger J, Fricker D, Miles R (2004) Interneuron diversity series: fast in, fast out-temporal and spatial signal processing in hippocampal interneurons. Trends Neurosci 27:30-40.

Komendantov AO, Ascoli GA (2009) Dendritic excitability and neuronal morphology as determinants of synaptic efficacy. J Neurophysiol 2009 101:1847-166.

Kumar SS, Buckmaster PS (2006) Hyperexcitability, interneurons, and loss of GABAergic synapses in entorhinal cortex in a model of temporal lobe epilepsy. J Neurosci 26:4613-4623.

Lee SY, Földy C, Szabadics J, Soltesz I (2011) Cell-type-specific CCK2 receptor signaling underlies the cholecystokinin-mediated selective excitation of hippocampal parvalbumin-positive fast-spiking basket cells. J Neurosci 31:10993-11002.

Leroy F, Lamotte d'Incamps B, Imhoff-Manuel RD, Zytnicki D (2014) Early intrinsic hyperexcitability does not contribute to motoneuron degeneration in amyotrophic lateral sclerosis. Elife doi: 10.7554/eLife.04046.

Lien CC, Jonas P (2003) Kv3 potassium conductance is necessary and kinetically optimized for high-frequency action potential generation in hippocampal interneurons. J Neurosci 23:2058-2068.

Lisman JE (1997) Bursts as a unit of neural information: making unreliable synapses reliable. Trends Neurosci 20:38-43.

London M, Schreibman A, Häusser M, Larkum ME, Segev I (2002) The information efficacy of a synapse. Nat Neurosci 5:332-340.

Lübke J, Frotscher M, Spruston N (1998) Specialized electrophysiological properties of anatomically identified neurons in the hilar region of the rat fascia dentata. J Neurophysiol 79:1518-1534.

Lydersen S, MW Fagerland MF, Laake P (2009) Recommended tests for association in 2 × 2 tables. Statistics in Medicine 28:1159-1175.

Mainen ZF, Sejnowski TJ (1996) Influence of dendritic structure on firing pattern in model neocortical neurons. Nature 382:363-366.

Masukawa LM, Benardo LS, Prince DA (1982) Variations in electrophysiological properties of hippocampal neurons in different subfields. Brain Res 242: 341–344.

Markram H, Toledo-Rodriguez M, Wang Y, Gupta A, Silberberg G, Wu C (2004) Interneurons of the neocortical inhibitory system. Nat Rev Neurosci 5:793-807.

Markram H, Muller E, Ramaswamy S, Reimann MW, Abdellah M, Sanchez CA, Ailamaki A, Alonso-Nanclares L, Antille N, Arsever S, Kahou GA, Berger TK, Bilgili A, Buncic N, Chalimourda A, Chindemi G, Courcol JD, Delalondre F, Delattre V, Druckmann S, Dumusc R, Dynes J, Eilemann S, Gal E, Gevaert ME, Ghobril JP, Gidon A, Graham JW, Gupta A, Haenel V, Hay E, Heinis T, Hernando JB, Hines M, Kanari L, Keller D, Kenyon J, Khazen G, Kim Y, King JG, Kisvarday Z, Kumbhar P, Lasserre S, Le Bé JV, Magalhães BR, Merchán-Pérez A, Meystre J, Morrice BR, Muller J, Muñoz-Céspedes A, Muralidhar S, Muthurasa K, Nachbaur D, Newton TH, Nolte M, Ovcharenko A, Palacios J, Pastor L, Perin R, Ranjan R, Riachi I, Rodríguez JR, Riquelme JL, Rössert C, Sfyrakis K, Shi Y, Shillcock JC, Silberberg G, Silva R, Tauheed F, Telefont M, Toledo-Rodriguez M, Tränkler T, Van Geit W, Díaz JV,

Walker R, Wang Y, Zaninetta SM, DeFelipe J, Hill SL, Segev I, Schürmann F (2015) Reconstruction and Simulation of Neocortical Microcircuitry. Cell 163:456-492.

McCormick DA, Connors BW, Lighthall JW, Prince DA (1985) Comparative electrophysiology of pyramidal and sparsely spiny stellate neurons of the neocortex. J Neurophysiol 54:782-806.

McNaughton BL, Barnes CA, O'Keefe J (1983) The contributions of position, direction, and velocity to single unit activity in the hippocampus of freely-moving rats. Exp Brain Res 52:41-49.

Mercer A, Trigg HL, Thomson AM (2007) Characterization of neurons in the CA2 subfield of the adult rat hippocampus. J Neurosci 27:7329-7338.

Mercer A, Botcher NA, Eastlake K, Thomson AM (2012) SP-SR interneurones: a novel class of neurones of the CA2 region of the hippocampus. Hippocampus 22:1758-1769.

Mott DD, Turner DA, Okazaki MM, Lewis DV (1997) Interneurons of the dentate-hilus border of the rat dentate gyrus: morphological and electrophysiological heterogeneity. J Neurosci 17:3990-4005.

O'Keefe J, Dostrovsky J (1971) The hippocampus as a spatial map. Preliminary evidence from unit activity in the freely-moving rat. Brain Res 34:171-175.

Pawelzik H, Hughes DI, Thomson AM (2002) Physiological and morphological diversity of immunocytochemically defined parvalbumin- and cholecystokinin-positive interneurones in CA1 of the adult rat hippocampus. J Comp Neurol 443:346-367.

Petilla Interneuron Nomenclature Group., Ascoli GA, Alonso-Nanclares L, Anderson SA, Barrionuevo G, Benavides-Piccione R, Burkhalter A, Buzsáki G, Cauli B, Defelipe J, Fairén A, Feldmeyer D, Fishell G, Fregnac Y, Freund TF, Gardner D, Gardner EP, Goldberg JH, Helmstaedter M, Hestrin S, Karube F, Kisvárday ZF, Lambolez B, Lewis DA, Marin O, Markram H, Muñoz A, Packer A, Petersen CC, Rockland KS, Rossier J, Rudy B, Somogyi P, Staiger JF, Tamas G, Thomson AM, Toledo-Rodriguez M, Wang Y, West DC, Yuste R (2008) Petilla terminology: nomenclature of features of GABAergic interneurons of the cerebral cortex. Nat Rev Neurosci 9:557-568.

Price CJ, Cauli B, Kovacs ER, Kulik A, Lambolez B, Shigemoto R, Capogna M (2005) Neurogliaform neurons form a novel inhibitory network in the hippocampal CA1 area. J Neurosci 25:6775-6786.

Rees CL, Wheeler DW, Hamilton DJ, White CM, Komendantov AO, Ascoli GA (2016) Graph theoretic and motif analyses of the hippocampal neuron type potential connectome. eNeuro 3. pii: ENEURO.0205-16.2016.

Rudy B, McBain CJ (2001) Kv3 channels: voltage-gated K^+ channels designed for high-frequency repetitive firing. Trends Neurosci 24:517-526.

Rudy JW, Sutherland RJ (1989) Configural association theory: The role of the hippocampal formation in learning, memory, and amnesia. Psychobiology 17: 129–144.

Rudy JW, Sutherland RJ (1995) Configural association theory and the hippocampal formation: an appraisal and reconfiguration. Hippocampus 5:375-389.

Savanthrapadian S, Meyer T, Elgueta C, Booker SA, Vida I, Bartos M (2014) Synaptic properties of SOM- and CCK-expressing cells in dentate gyrus interneuron networks. J Neurosci 34:8197-8209.

Sciamanna G, Wilson CJ (2011) The ionic mechanism of gamma resonance in rat striatal fast-spiking neurons. J Neurophysiol 106:2936-2949.

Smith M, Perrier JF (2006) Intrinsic properties shape the firing pattern of ventral horn interneurons from the spinal cord of the adult turtle. J Neurophysiol 96:2670-2677.

Song C, Xu XB, He Y, Liu ZP, Wang M, Zhang X, Li BM, Pan BX (2013) Stuttering interneurons generate fast and robust inhibition onto projection neurons with low capacity of short term modulation in mouse lateral amygdala. PLoS One 8:e60154.

Spruston N, Lübke J, Frotscher M (1997) Interneurons in the stratum lucidum of the rat hippocampus: an anatomical and electrophysiological characterization. J Comp Neurol 385:427-440.

Tamas G, Lorincz A, Simon A, Szabadics J (2003) Identified sources and targets of slow inhibition in the neocortex. Science 299:1902-1905.

Tricoire L, Pelkey KA, Erkkila BE, Jeffries BW, Yuan X, McBain CJ (2001) A blueprint for the spatiotemporal origins of mouse hippocampal interneuron diversity. J Neurosci 31:10948-10970.

Wheeler DW, White CM, Rees CL, Komendantov AO, Hamilton DJ, Ascoli GA (2015) Hippocampome.org: a knowledge base of neuron types in the rodent hippocampus. Elife doi: 10.7554/eLife.09960.

Xu W, Morishita W, Buckmaster PS, Pang ZP, Malenka RC, Südhof TC (2012) Distinct neuronal coding schemes in memory revealed by selective erasure of fast synchronous synaptic transmission. Neuron 73:990-1001.

Zemankovics R, Káli S, Paulsen O, Freund TF, Hájos N (2010) Differences in subthreshold resonance of hippocampal pyramidal cells and interneurons: the role of h-current and passive membrane characteristics. J Physiol 588:2109-2132.

Zhao ML, Wu CF (1997) Alterations in frequency coding and activity dependence of excitability in cultured neurons of *Drosophila* memory mutants. J Neurosci 17:2187-2199.

Legends

Figure 1. Classification of firing pattern elements.

Figure 2. Firing pattern elements observable in hippocampal neurons *in vitro*. ISI - interspike interval, PFS – post firing silence, sDW – slow depolarization wave, sAHP – slow afterhyperpolarization. Electrophysiological recording modified from Lübke et al. (1998) (D), Vida et al. (1998) (ASP), Pawelzik et al. (2002) (RASP), Hamam et al. (2002) (TSTUT), Chevaleyre and Seigelbaum (2010) (TSWB), Mercer et al. (2012) (SLN), Mott et al. (1997) (NASP), Fuentealba et al. (2010) (PSTUT), and Golomb et al. (2006) (PSWB, spontaneous bursting in Ca^{2+} free ACSF).

Figure 3. Examples of fitting of spiking activity with linear regression and piecewise linear regression models. **A.** Responses to current injection of a DG aspiny interneuron with axonal projection to the inner molecular layer (AIPRIM in Hippocampome.org) (Modified from Lübke et al., 1998). **B.** Fitting of digitized experimental data with different models.

1 parameter fit is a constant function Y=2.78;

2 parameter fit is a linear function Y=0.017X+1.67;

3 parameter fit is a piecewise linear function $Y = \begin{cases} 0.031X + 1.27 & if\ X < 74.9 \\ 3.58 & if\ X \geq 74.9 \end{cases}$;

4 parameter fit is a piecewise linear function $Y = \begin{cases} 0.033X + 1.23 & if\ X < 61.3 \\ 0.006X + 2.87 & if\ X \geq 61.3 \end{cases}$.

Based on *p*-values, the firing pattern was identified as adapting-non-adapting spiking (ASP.NASP): $p_{2,1} < 0.05$ ($p_{2,1} = 1.26 \cdot 10^{-10}$), $p_{3,2} < 0.025$ ($p_{3,2} = 2.7 \cdot 10^{-3}$), $p_{4,3} > 0.016$ ($p_{4,3} = 5.5 \cdot 10^{-2}$). $p_{2,1}$, $p_{3,2}$, $p_{4,3}$ – p-values of differences between 2 parameter fit and 1 parameter fit, 3 parameter fit and 2 parameter fit, 4 parameter fit and 3 parameter fit, respectively.

Figure 4. Flow chart of general procedure of firing pattern identification.

Figure 5. Identified firing patterns and firing pattern phenotypes complexity of 89 neuron types (A and B) with 42 subtypes (B). Online matrix: hippocampome.org/firing_patterns. Green and red cell type/sybtype names denote excitatory (e) and inhibitory (i) neurons, respectively. FPP is firing pattern phenotype. The numbers in the brackets correspond to the order in which the cell types were presented in the Hippocampome (ver. 1.0).

Figure 6. Occurrence of firing patterns, firing pattern elements and firing pattern phenotypes among the hippocampal formation neuron types. **A**. Distribution of 23 firing

patterns; total numbers are shown above the bars. **B**. Distribution of 9 firing pattern elements; total numbers are in parentheses below and percentages of occurrence among 89 cell types are above the bars. **C**. Complexity of firing pattern phenotypes; percentages and ratios indicate occurrences of phenotypes of different complexity among 122 cell types. **D**. Relationships between firing pattern elements in the firing patterns of hippocampal neuron types. Numbers of cell types with distinctive firing patterns are indicated. 51+1 denotes number of cell types with ASP. and ASP.ASP. firing, respectively.

Figure 7. Eleven firing pattern phenotypes of 116 neuron types/subtypes. Simple adapting firing pattern phenotype is not unique (see *Results*). **A**. Hierarchical tree resulting from two-step clustering of weighted firing pattern elements with representative examples of cell types/subtypes which belong to corresponding firing pattern phenotype. **B**. Relative proportions of firing pattern phenotypes among neuron types/subtypes. Green and red numbers represent excitatory and inhibitory cell types/subtypes as they numerated in Fig. 5. **C**. Percentage of occurrence of firing pattern elements in firing pattern phenotypes. **D**. Distribution of firing pattern phenotypes among sub-regions of the hippocampal formation.

Figure 8. Hippocampome.org enables searching neuron types by neurotransmitter; axon, dendrite, and soma locations; molecular expression; electrophysiological parameters; input/output connectivity; firing patterns, and firing pattern parameters. **A**.

Sample query for cabining-negative neuron types with axons in CA1 stratum pyramidale, AP_{width} <0.96 ms, PSTUT firing, and ratio maximum ISI to the next ISI is more than 10. Numbers in parentheses indicate the number of neuron types with the selected property or combination of properties. **B**. Search results are linked to the neuron page(s). **C**. The neuron page is linked to the firing pattern evidence page. **D**. All firing pattern parameters and ISIs can be displayed.

Figure 9. Relationships between the width of action potentials (AP_{width}) and minimum of interspike intervals (ISI_{min}) for 84 neuron types and subtypes. **A.** AP_{width} - ISI_{min} scatter diagram with results of linear regression. Green triangles and red circles indicate excitatory and inhibitory neurons, respectively. Dashed orange lines: horizontal line separates neurons with slow spikes from neurons with fast and moderate spikes; vertical lines (*w1* and *w2*) separate neurons with narrow, medium and wide action potentials. Black lines: solid line shows linear fitting for slow spike neurons with a function Y = - 26.72X + 76.42 (R^2=0.83); dashed lie shows general linear fitting for fast and moderate spike neurons with a function Y = 13.79X - 0.05 (R^2=0.52). **B**. AP_{width} histogram. **C**. ISI histogram.

Table 1. Principles of classification of firing pattern elements

Abbreviations**:** a_1 – slope of linear fitting for normalized ISIs *vs* normalized time; *DF* – delay factor; f_{min} – minimum frequency of stuttering or bursting; F_{pre}, F_{post} and F_{PSTUT} – ISI comparison factors, ISI_{max} –maximum interspike interval; $p_{2,1}$ – *p*-value for differences

between two- and one-parameter linear fitting; $p_{3,2}$ – *p*-value for differences between three- and two-parameter linear fitting; *PFS* – post firing silence; *SF* – silence factor; S_{RASP} – slope of linear fitting of rapid transient; *SWA* – slow wave amplitude; SWA_{min} – minimum slow wave amplitude.

Table 2. Occurrences of completed firing patterns in hippocampal and other neurons

NASP - HICAP(Mott et al. 1997, Fig. 11A); **PSTUT** - CA1 Neurogliaform (Fuentealba et al. 2010, Fig.5B); **PSWB** - CA3 Pyramidal (Bilkey and Schwartzkroin 1990, Fig. 1a); **ASP.NASP** - CA3 Basket-CCK (Gulyás et al. 2010, Fig. 1b, right); **ASP.SLN** – EC MEC LV Pyramidal (Canto and Witter 2012b, Fig.10C7); **ACSP.NASP** - ventral horn interneuron of turtle (Smith and Perrier 2006, Fig. 2D); **RASP.NASP** – EC LV Deep Pyramidal (Hamam et al. 2000, Fig.3C); **RASP.SLN** – CA1 Radiatum Giant (**Bullis et al. 2007**, Fig.5A); **TSTUT.NASP** - EC LV Deep Pyramidal (Hamam et al. 2002, Fig.5E); **TSTUT.PSTUT** - CA1 (Price et al. 2005, Fig.3A2); **TSUT.SLN** – CA2 SP-SR (Mercer et al. 2012; Fig. 3A); **TSWB.NASP** - CA1 Pyramidal (Zemankovics et al. 2009, Fig. 1B); **TSWB.SLN** - CA3 Pyramidal (Hemond et al. 2008, Fig. 4); **D.NASP** – DG Neurogliaform (Armstrong et al. 2011, Fig.3A, top trace); **D.PSTUT** - CA2 Basket (Mercer et al. 2007, Fig. 5B)**; D.PSWB** - cultured *rutabaga* mutant giant neuron of *Drosophila* (Zhao and Wu 1997, Fig.7, *top left*); **D.ASP.SLN -** neuron in external lateral subnucleus of lateral parabrachial nucleus (Hayward and Felder 1999, Fig.3A, top); **D.ACSP.NASP** – motoneuron (Leroy et al. 2014, Figure 1-figure supplement 1B); **D.RASP.NASP** - CA3 LMR-Targeting (Ascoli et al. 2009, Fig. 1A); **D.TSUT.SLN** -

striatal fast-spiking neuron (Sciamanna and Wilson 2011, Fig. 1C); **D.TSWB.NASP** - CA1 Axo-Axonic (Buhl et al. 1994, Fig. 5D).

Illustrations and Tables

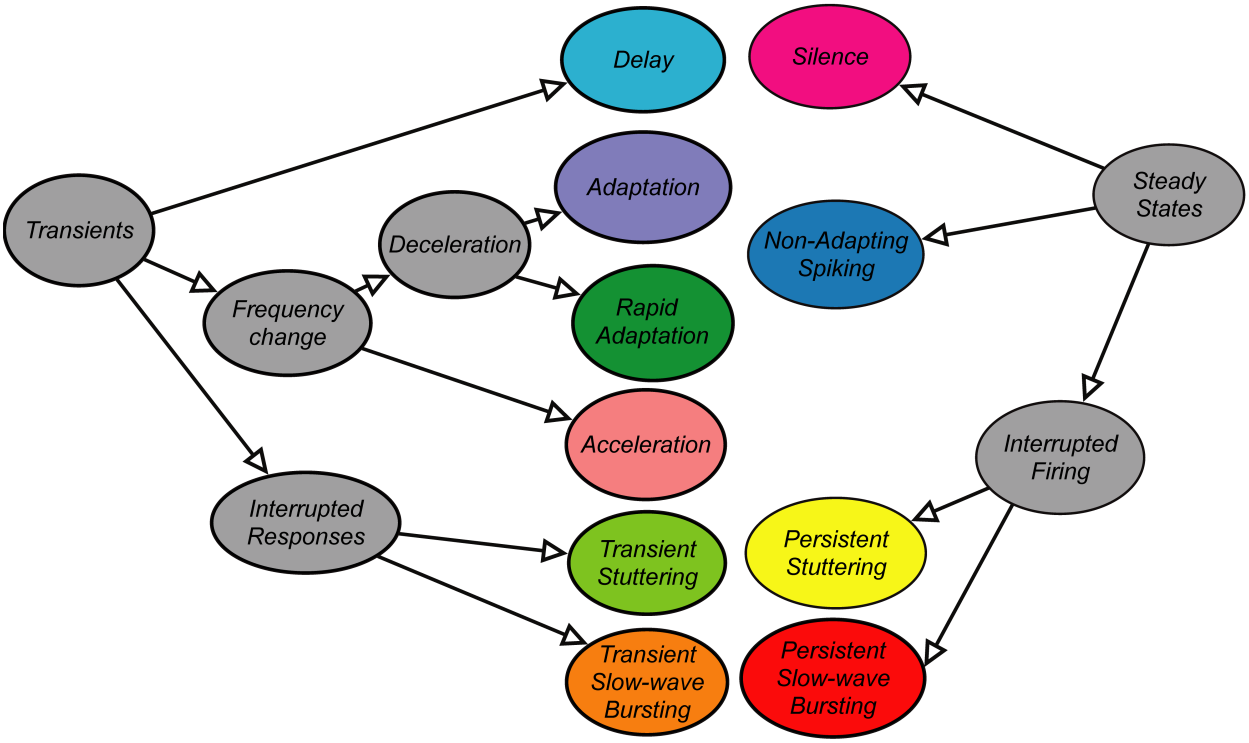

Figure 1.

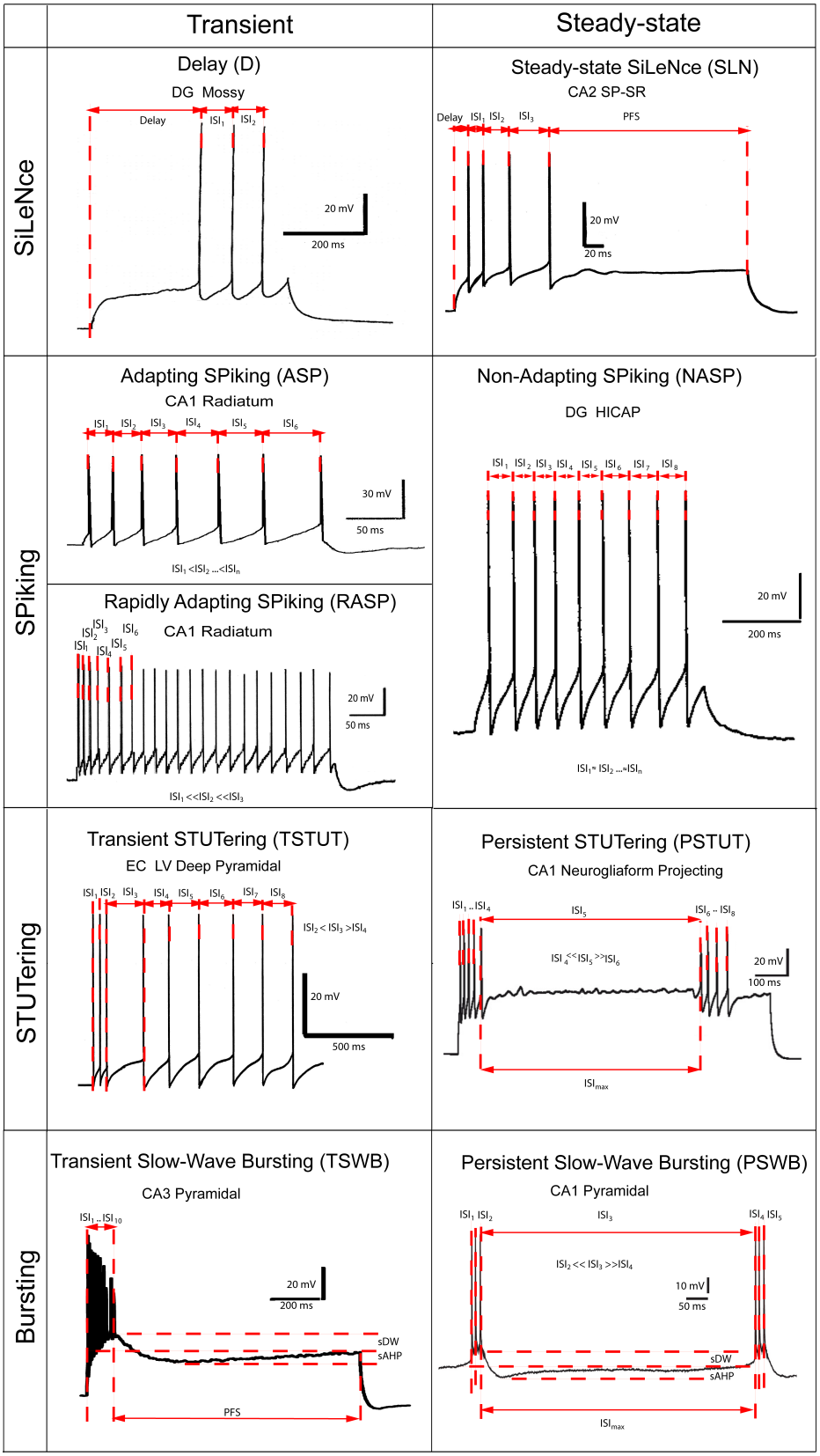

Figure 2.

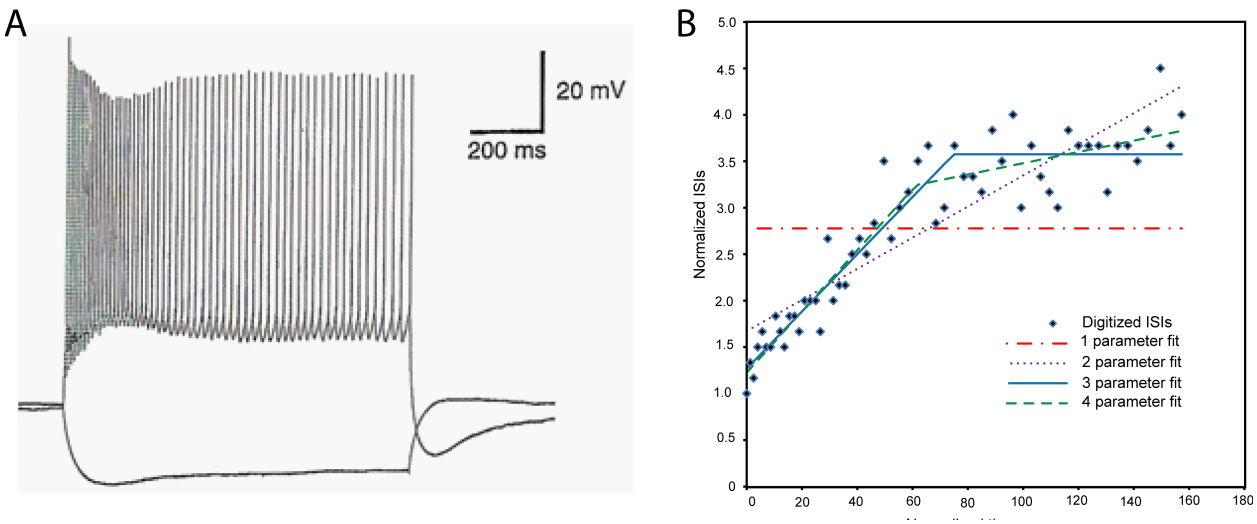

Figure 3.

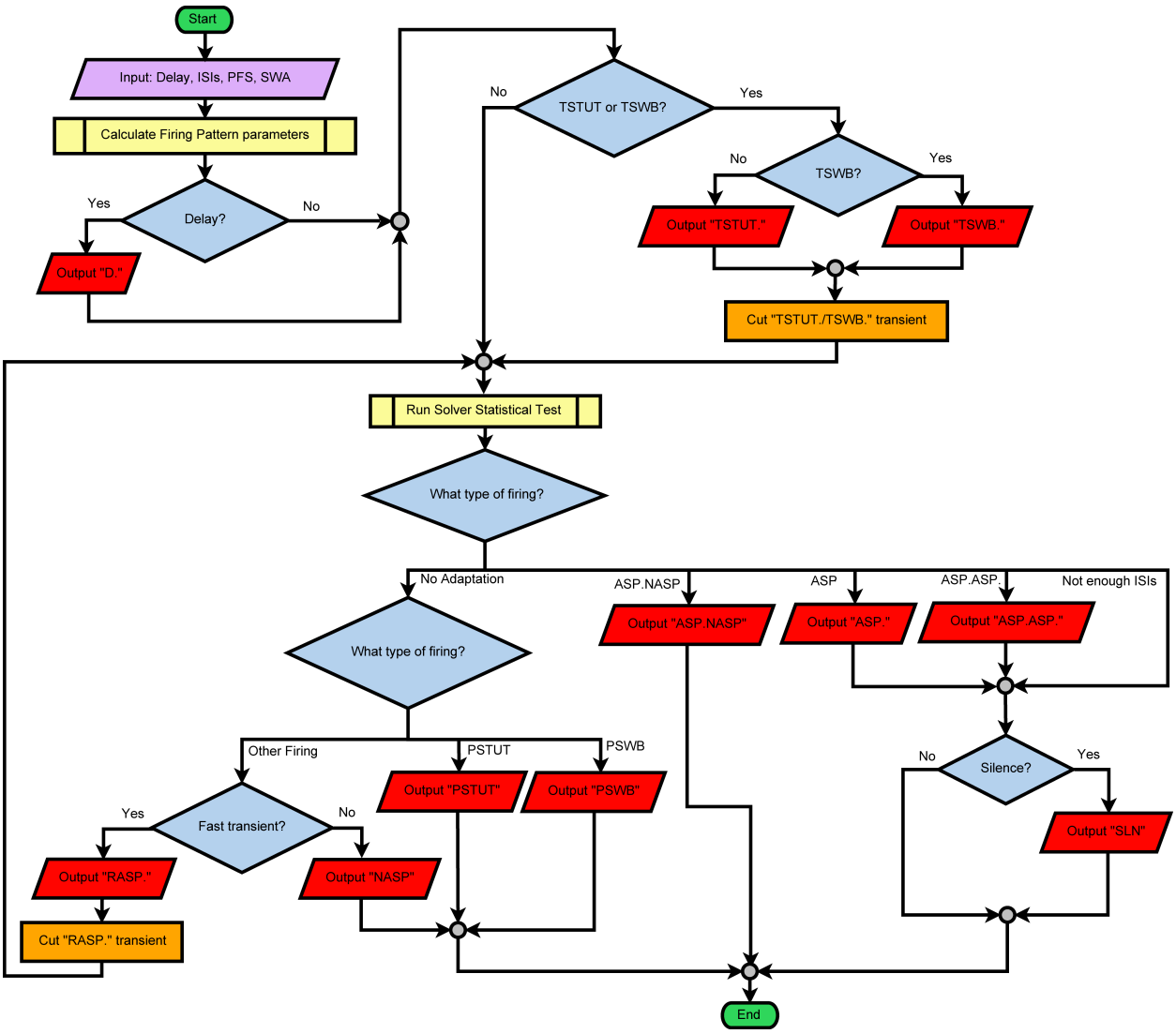

Figure 4.

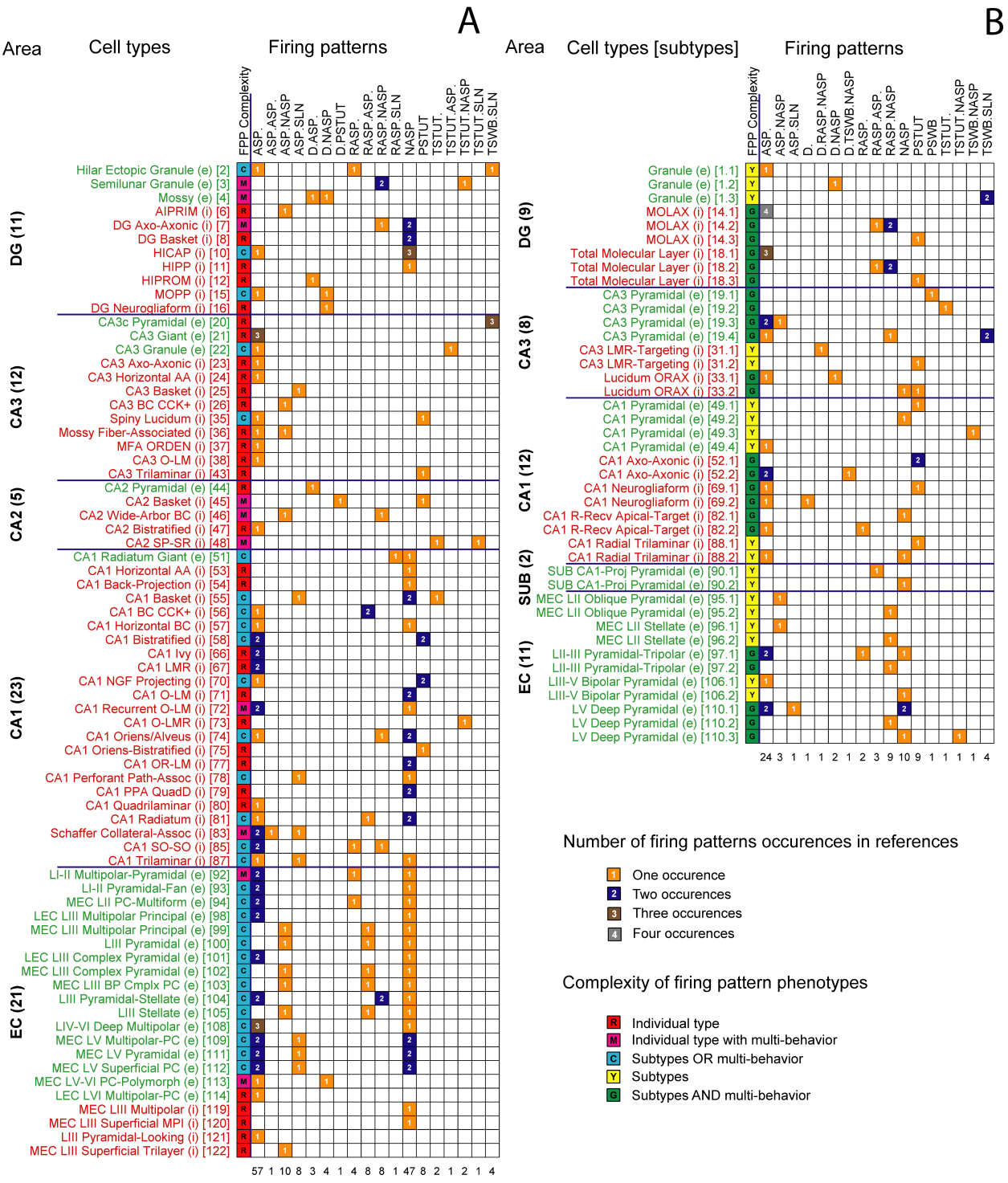

Figure 5.

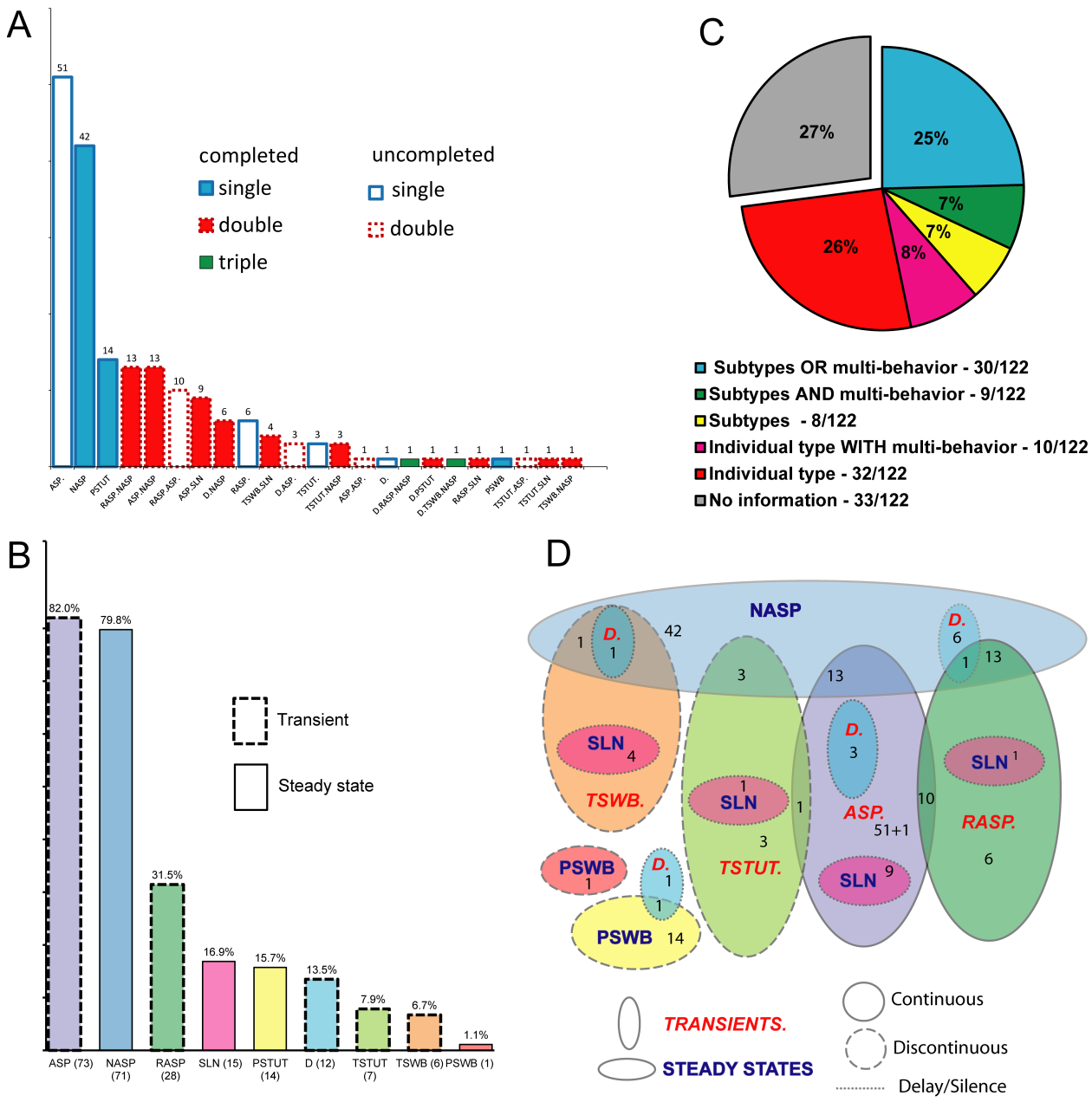

Figure 6.

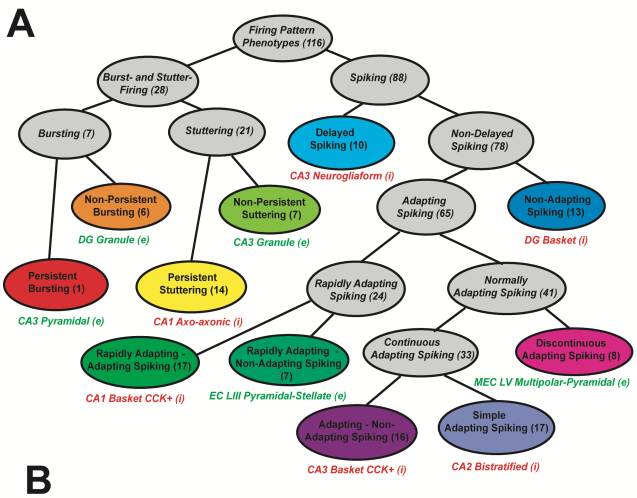

C

	Firing Pattern Elements								
Firing Pattern Phenotype	ASP	D	RASP	NASP	PSTUT	PSWB	SLN	TSTUT	TSWB
Persistent Bursting (1)	0%	0%	0%	0%	0%	100%	0%	0%	0%
Non-Persistent Bursting (6)	50%	17%	33%	50%	0%	0%	67%	0%	100%
Persistent Stuttering (14)	23%	8%	0%	8%	100%	0%	0%	0%	0%
Non-Persistent Stuttering (7)	29%	0%	14%	57%	0%	0%	29%	100%	0%
Delayed Spiking (10)	70%	100%	10%	70%	0%	0%	0%	0%	0%
Non-Adapting Spiking (13)	0%	0%	0%	100%	0%	0%	0%	0%	0%
Adapting - Non-Adapting Spiking (16)	100%	0%	0%	100%	0%	0%	0%	0%	0%
Simple Adapting Spiking (17)	100%	0%	0%	0%	0%	0%	0%	0%	0%
Discontinuous Adapting Spiking (8)	100%	0%	0%	75%	0%	0%	100%	0%	0%
Rapidly Adapting - Non-Adapting Spiking (7)	0%	0%	100%	100%	0%	0%	14%	0%	0%
Rapidly Adapting - Adapting Spiking (17)	100%	0%	100%	82%	0%	0%	0%	0%	0%

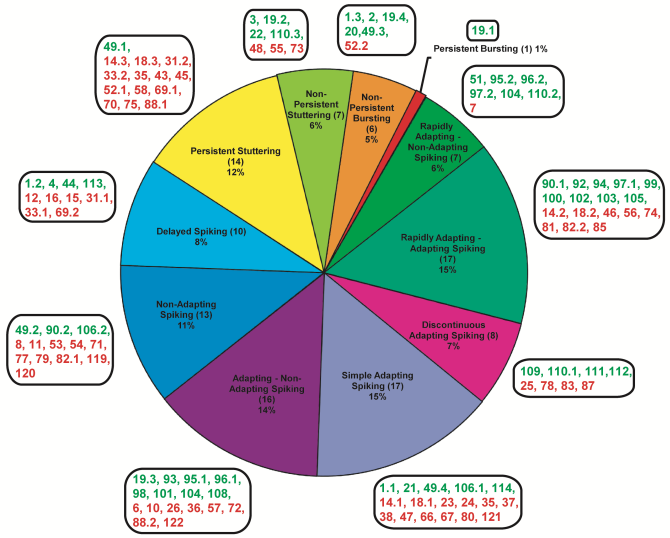

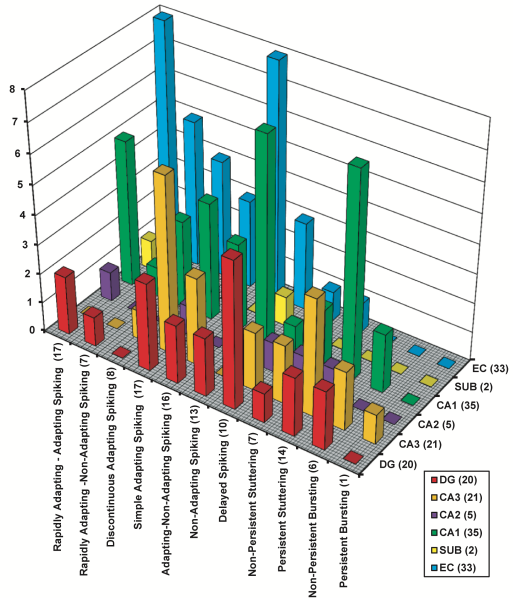

Figure 7.

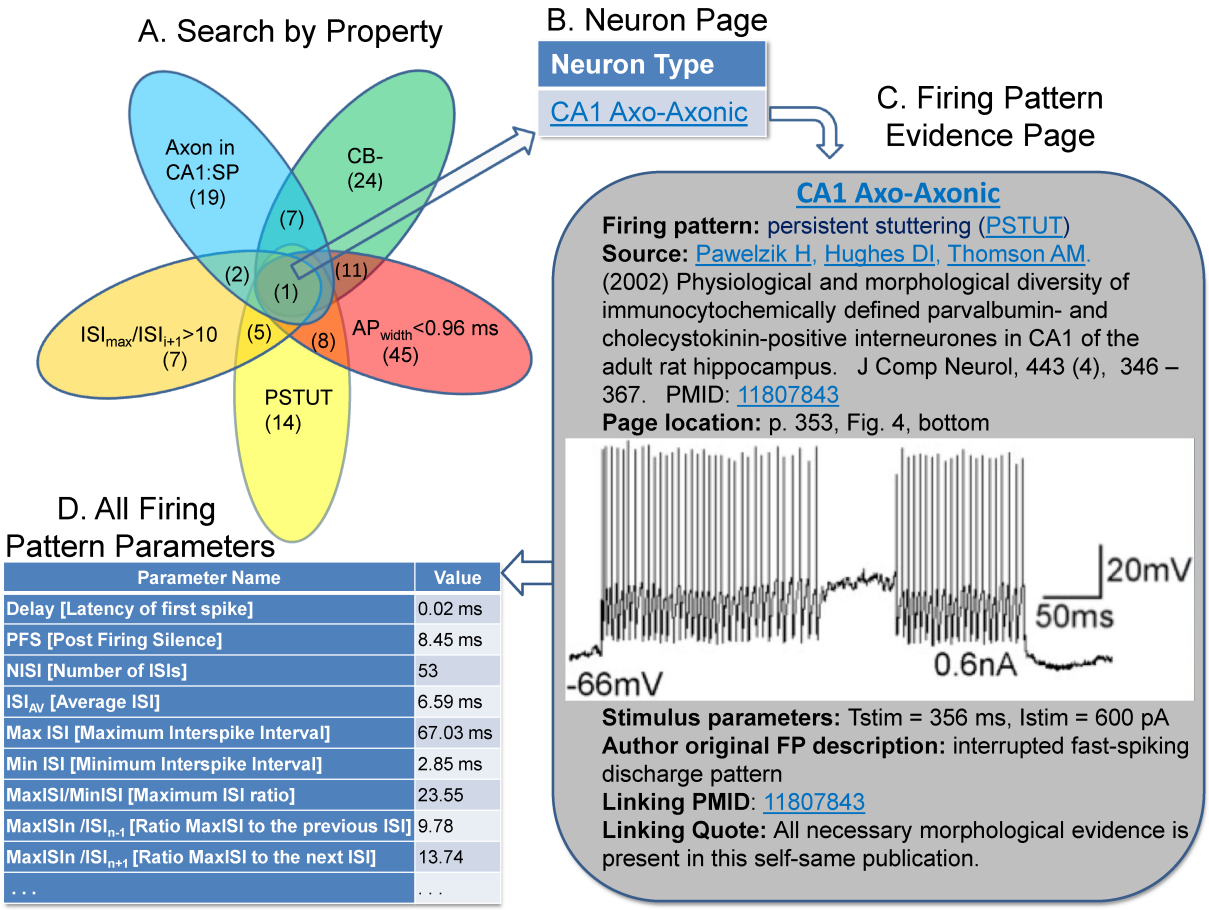

Parameter Name	Value
Delay [Latency of first spike]	0.02 ms
PFS [Post Firing Silence]	8.45 ms
NISI [Number of ISIs]	53
ISI_{AV} [Average ISI]	6.59 ms
Max ISI [Maximum Interspike Interval]	67.03 ms
Min ISI [Minimum Interspike Interval]	2.85 ms
MaxISI/MinISI [Maximum ISI ratio]	23.55
MaxISIn /ISI_{n-1} [Ratio MaxISI to the previous ISI]	9.78
MaxISIn /ISI_{n+1} [Ratio MaxISI to the next ISI]	13.74
. . .	. . .

Figure 8.

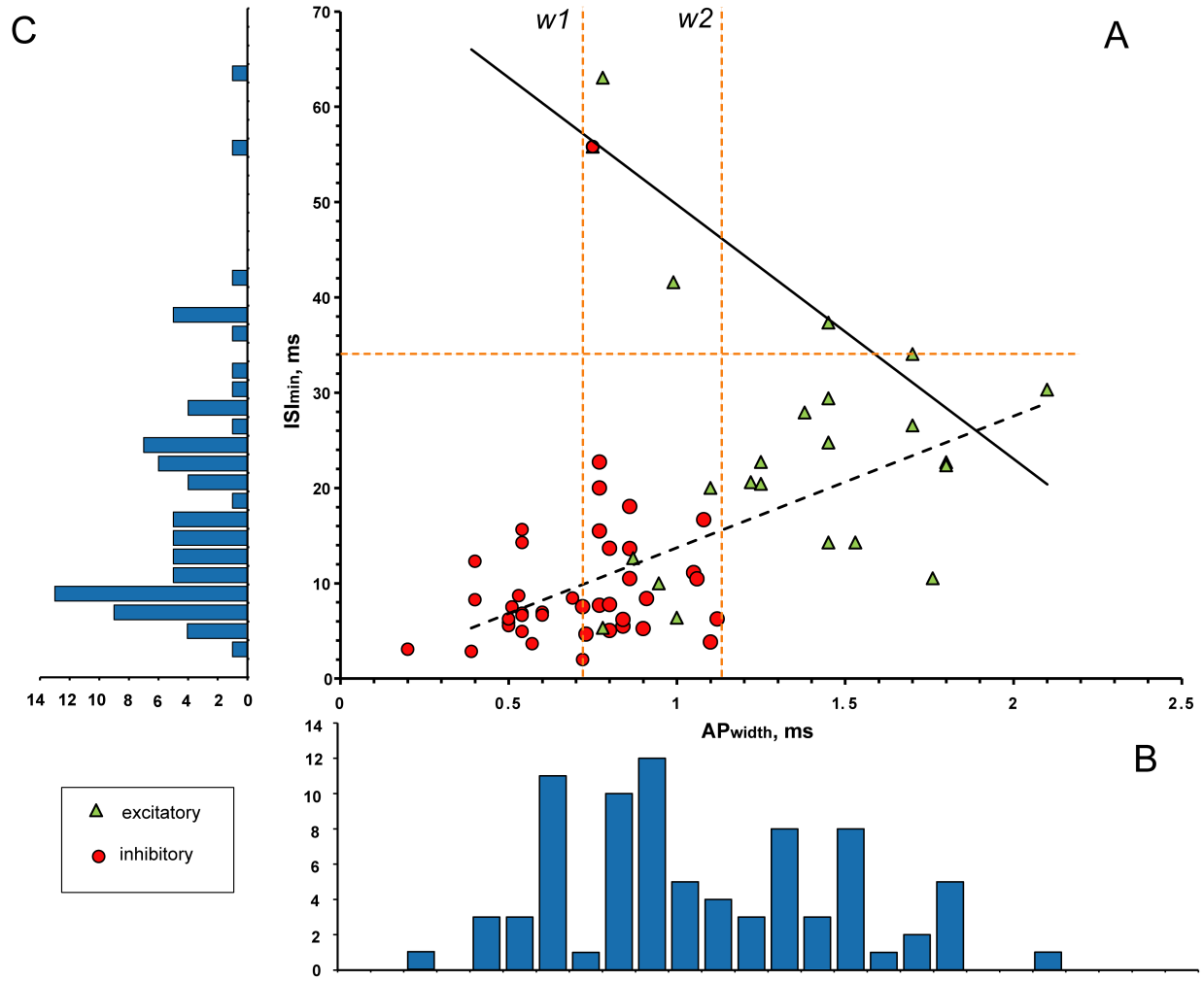

Figure 9.

Table 1. Principles of classification of firing pattern elements

Firing pattern element		Transient responses	Steady-state responses	Characteristics of responses	Values of parameters
Silence		Delayed (D)		$Delay > DF\frac{ISI_1 + ISI_2}{2}$	$DF = 2$
			SiLeNce (SLN)	$PFS > SF\frac{ISI_n + ISI_{n-1}}{2}$ $PFS > SF * ISI_{\max}$	$SF = 2$
Spiking		Adapting Spiking (ASP)		$ISI_1 < ISI_2 < ISI_n$; to compare 2 parameter fit $(Y=a_1X+b_1)$ and 3 parameter fit $(Y=a_1X+b_1; Y=b_2)$	$p_{2,1}<0.05$ $p_{3,2}>0.025$ $a_1 > 0.003$
		Rapidly Adapting Spiking (RASP)		$ISI_1 << ISI_2 << ISI_3$ $Y = a_1X + b_1$ $a_1 > S_{RASP}$	$S_{RASP} = 0.2$
		Accelerating Spiking (ACSP)		$ISI_1 > ISI_2 > ISI_n$; to compare 2 parameter fit $(Y=a_1X+b_1)$ and 3 parameter fit $(Y=a_1X+b_1; Y=b_2)$	$p_{2,1}<0.05$ $p_{3,2}>0.025$ $a_1 < -0.003$
			Non-Adapting Spiking (NASP)	$ISI_1 \approx ISI_2 \ldots \approx ISI_n$; to compare 1 parameter fit $(Y=b_1)$ and 2 parameter fit $(Y=a_1X+b_1)$	$p_{2,1}>0.05$
Interrupted	Stuttering	Transient STUTering (TSTUT)		$ISI_i > F_{pre} * ISI_{i-1}$ $ISI_i > F_{post} * ISI_{i+1}$ $\frac{\sum_{j=i}^{n} ISI_j}{n-j} > F_{pre}\frac{\sum_{j=1}^{i-1} ISI_j}{j}$ (T1.1) $\forall j < i-1: \frac{1}{ISI_j} > f_{\min}$	$F_{pre}=2.5$ $F_{post}=1.5$ $f_{\min}= 25$ Hz $i=2,3,4$
			Persistent STUTering (PSTUT)	$\frac{ISI_i^{\max}}{ISI_{i-1}} + \frac{ISI_i^{\max}}{ISI_{i+1}} > F_{PSTUT}$ (T1.2)	$F_{PSTUT}=5$
	Slow-Wave Bursting	Transient Slow-Wave Bursting (TSWB)		Inequalities T1.1, $SWA > SWA_{\min}$	$F_{pre}=2.5$ $F_{post}=1.5$ $f_{\min}=25$ Hz $i=2,3,4$ $SWA_{\min} = 5$ mV
			Persistent Slow-Wave Bursting (PSWB)	Inequality T1.2, $SWA > SWA_{\min}$	$F_{PSTUT}=5$ $SWA_{\min} = 5$ mV

Table 2. Occurrences of completed firing patterns in hippocampal and other neurons

			Steady States			
			NASP	PSTUT	PSWB	SLN
	-	-	**NASP** DG HICAP	**PSTUT** CA1 Neurogliaform	**PSWB** CA3 Pyramidal	-
Transients	-	ASP	**ASP.NASP** CA3 Basket-CCK	ASP.PSTUT	ASP.PSWB	**ASP.SLN** EC MEC LV Pyramidal
	-	ACSP	**ACSP.NASP** Ventral horn turtle interneuron	**ACSP.PSTUT**	ACSP.PSWB	**ACSP.SLN**
	-	RASP	**RASP.NASP** EC LV Deep Pyramidal	RASP.PSTUT	RASP.PSWB	**RASP.SLN** CA1 Radiatum Giant
	-	TSTUT	**TSTUT.NASP** EC LV Deep Pyramidal	**TSTUT.PSTUT**	TSTUT.PSWB	**TSTUT.SLN** CA2 SP-SR
	-	TSWB	**TSWB.NASP** CA1 Pyramidal	TSWB.PSTUT	**TSWB.PSWB**	**TSWB.SLN** CA3 Pyramidal
	D	-	**D.NASP** DG Neurogliaform	**D.PSTUT** CA1 Bistratified	**D.PSWB** Giant neuron of *Drosophila*	-
	D	ASP	**D.ASP.NASP**	D.ASP.PSTUT	D.ASP.PSWB	**D.ASP.SLN** Lateral parabrachial nucleus
	D	ACSP	**D.ACSP.NASP** Motoneuron	**D.ACSP.PSTUT**	D.ACSP.PSWB	**D.ACSP.SLN**
	D	RASP	**D.RASP.NASP** CA3 LMR-Targeting	D.RASP.PSTUT	D.RASP.PSWB	**D.RASP.SLN**
	D	TSTUT	**D.TSTUT.NASP**	**D.TSTUT.PSTUT**	D.TSTUT.PSWB	**D.TSTUT.SLN** Striatal fast-spiking
	D	TSWB	**D.TSWB.NASP** CA1 Axo-Axonic	D.TSWB.PSTUT	**D.TSWB.PSWB**	**D.TSWB.SLN**

NASP	observed in hippocampal neurons
PSWB	observed in other neurons
D.ASP.NASP	not found but possible
TSWB.PSTUT	improbable
-	impossible (no firing)

Box 1. Correlations between electrophysiological, molecular, morphological and firing pattern data in the Hippocampome

1) There is no neuron type that is neuropeptide Y (**NPY**) positive or has low value of membrane time constant (τ_m) and becomes silent (**SLN**) after short firing discharge ($p<0.014$, $n=29$ and $p<0.024$, $n=32$, respectively).
2) Of 25 cell types that have **wide APs**, only one (EC LV-VI pyramidal-polymorphic) can show delayed (**D.**) firing ($p<0.021$, $n=25$), and only one (EC LVI multipolar-pyramidal) does show non-adapting spiking (**NASP**) ($p<0.021$, $n=25$).
3) Only one (CA1 Schaffer collateral-associated) out of the 35 neuron types with low-threshold (low $\mathbf{V_{thresh}}$), only two (CA3 granule and EC LVI multipolar pyramidal) out of the 23 neuron types with low values for **slow AHP,** and two out of 33 cell types exist that have low values for fast after hyperpolarization (**fAHP**), which do not demonstrate non-adapting spiking (**NASP**) ($p<0.02$, $n=35$, $p<0.016$, $n=23$ and $p<0.007$, $n=33$, respectively).
4) While positive expression of cholecystokinin (**CCK**) tends to coincide with adapting spiking (**ASP.**) ($p<0.011$, $n = 26$), neuron types with high input resistance ($\mathbf{R_{in}}$) do not demonstrate adapting spiking (**ASP.**) ($p<0.012$, $n=35$).
5) Of the 25 neuron types that have **narrow APs**, only one (CA1 basket CCK+) of the 29 cell types with high value of hyperpolarization-induced **sag** potential, only one cell (CA3 pyramidal cell), and of the 33 neuron types that have high values for fast after-hyperpolarization (**fAHP**), only two (DG semilunar granule cell and CA1 basket CCK+ cells) display rapidly adapting spiking (**RASP.**) ($p<0.008$, $n=25$, $p<0.022$, $n=29$ and $p<0.018$, $n=33$, respectively).
6) Of the 33 **glutamatergic** neuron types (33/89), only CA1 pyramidal cell demonstrates persistent stuttering (**PSTUT**) ($p<0.013$, $n=89$).
7) Only one (CA1 axo-axonic) out of 89 neuron types exist that are not **projecting** (61/89) and demonstrate transient slow-wave bursting (**TSWB**.) ($p<0.026$, $n=89$).

The p values and sample sizes (n) are computed using Bernard's exact test for 2 × 2 contingency tables (see Materials and methods).